https://doi.org/10.15407/ujpe63.3.226

A. SRIBOONRUANG,[1,2] T. KUMPIKA,[2] W. SROILA,[2] E. KANTARAK,[2] P. SINGJAI,[2,3] W. THONGSUWAN[2,3]

[1] Graduate School Chiang Mai University
(239, Huay Kaew Road, Muang, Chiang Mai 50200, Thailand)
[2] Department of Physics and Materials Science, Faculty of Science, Chiang Mai University
(239, Huay Kaew Road, Muang, Chiang Mai 50200, Thailand)
[3] Materials Science Research Center, Faculty of Science, Chiang Mai University
(239, Huay Kaew Road, Muang, Chiang Mai 50200, Thailand; e-mail: wiradej.t@cmu.ac.th)

SUPERHYDROPHOBICITY/SUPERHYDROPHILICITY TRANSFORMATION OF TRANSPARENT PS-PMMA-SiO_2 NANOCOMPOSITE FILMS

A transparent superhydrophobic nanocoating with high water contact angle (>150°) was successfully prepared by a simple dip coating method. The coating solutions were prepared by the dissolution of polystyrene (PS) and poly(methyl methacrylate) (PMMA) in toluene. Fumed silica (SiO_2) was then added to increase the roughness of the coating. The annealing treatment conditions were investigated to optimize the water contact angle. The heat treatment conditions and other factors were studied systematically to optimize the transmission and the contact angle of water on the films. The results have shown that the films increase with the annealing temperature. The superhydrophobicity of films is observed only in PS-consisted films after the annealing at 200 °C. The superhydrophobic/superhydrophilic transformation was achieved at the annealing temperature higher than 200 °C due to the decay of the polymer into hydrophilic monomers.

K e y w o r d s: superhydrophobicity, superhydrophilicity, SiO_2, PMMA, PS, films, dip coating.

1. Introduction

The wettability of a solid surface is determined by measuring the water contact angle (WCA) and sliding angle (SA). Surfaces with WCA in the range of 10–90 degree are hydrophilic, whereas surfaces with WCA less than 10 degree are superhydrophilic. On the other hand, surfaces with contact angle in the range of 90–150 degree are hydrophobic, whereas surfaces with WCA higher than 150 degree and SA less than 10 degree are considered to be superhydrophobic. The WCA are commonly used to describe opposite effects of the behavior of water on a solid surface. The hydrophilic surface allows water to spread completely across the surface, whereas the static water droplet on a hydrophobic surface is almost spherical and easily repellent.

Recently, both superhydrophilic and superhydrophobic surfaces have attracted an enormous amount of interest. Superhydrophilic surfaces are investigated for their potential to provide antifogging, antifouling [1], and photocatalytic properties [2]. Superhydrophobic surfaces have found numerous potential practical applications such as self-cleaning surfaces [3], corrosion resistant ones [4], and those preventing the adhesion of snow [5]. Conventionally, superhydrophobic surfaces have been obtained by enhancing a low surface energy and a hierarchical micrometer/nanometer-sized roughness. Many methods have been developed to produce appropriated wetting properties of surfaces, for example: low-pressure plasma [6], lithographic patterning [7], chemical vapor deposition [8], and sol-gel technique [9]. Most of these methods are expensive or cannot be easily scale-up. In addition, even though a great number of the procedures of preparation of superhydrophobic or superhydrophilic surfaces have been reported, the reports on superhydrophobic to superhydrophilic transforms have seldom been seen. D.L. Torres *et al.* [10] prepared superhydrophilic films, by using poly(allylaminehydrochloride) (PAH) and poly(sodium phosphate) (PSP) combined by the layer-by-layer self-assembly technique. The

films were functionalized to transform them into superhydrophobic by the chemical vapor deposition (CVD). J. Liang *et al.* [11] demonstrated superhydrophilic/superhydrophobic transforms on titanium surfaces. The Ti substrates were anodized to produce superhydrophilic surface, and further the fluorinated modification makes the surface upper hydrophobic. Y.H. Lin and co-workers [12] reported a superhydrophilic/superhydrophobic surface on glass substrates. The film consisted of the adhesion/body/top layer structure was prepared, by using SiO_2 nanoparticles and polyelectrolytes. Superhydrophilic/superhydrophobic transforms can be achieved, by using the appropriate volume ratio of silica nanoparticles in a solution for the body layer deposition, with and without silane treatment in the fabrication process. In the present work, we offer a simple economical method to fabricate superhydrophilic/superhydrophobic surfaces, by using the dip coating on a glass substrate. Here, hydrophilic silica nanoparticles were chosen as a coating material due to its non-toxicity, high thermal and mechanical stabilities, and low cost. PS/PMMA were used as a modifying agent. We investigated effects of the annealing temperature on morphological, structural, and especially wetting properties of the coated films. The result indicated that the coated films could be transformed from the hydrophilic state to both superhydrophobic and superhydrophilic forms depending on the annealing temperature. This adjustable wetting property opens an opportunity to use these films as candidates in actual industrial applications.

2. Materials and Methods

2.1. Materials

Silica fume powder (0.007 μm), PMMA, and PS were purchased from Sigma-Aldrich, U.S.A. The chemicals used are toluene (RCl Labscan) and ethanol (EMSURE®, Absolute for analysis).

2.2. Sample Preparation

0.2 g of PS and PMMA were added to 20 ml of toluene and then stirred at 100 °C for 30 min to form solutions A and B, respectively. The solution C was obtained by mixing solutions A and B in the 1:1 volume ratio. 0.5 g of SiO_2 nanoparticles were then mixed into all solutions and stirred for 30 min at room temperature. Glass substrates were sonically cleaned in acetone, distilled water, and ethanol and then dried by the nitrogen gas blowing. The substrates were immersed into the solutions for 5 s and slowly removed and dried in air for 6 h. Finally, these films were then annealed at 100–500 °C for 2 h.

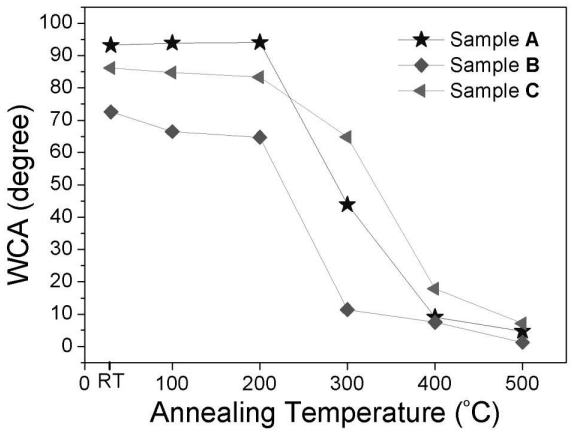

Fig. 1. Relationship between WCA of the coated films and the annealing temperature

2.3. Sample Characterization

Water contact angles (WCA) were measured at room temperature. The surface morphology was characterized, by using SEM images (JEOL JSM-6335F). The chemical composition was analyzed by an energy dispersive spectroscopy (EDS) drvice equipped with the same SEM. The root mean square (RMS) roughness was examined, by using an AFM in the tapping mode (Digital Instruments, Inc.) at room temperature. The Raman spectra were recorded, by using 514.5 nm argon ion lasers at room temperature (Jobin Yvon Horiba T64000).

3. Results and Discussion

WCAs of samples A, B, and C were measured in relation to the annealing temperatures, as shown in Fig. 1. At room temperature, WCAs of samples A, B, and C were 93, 86, and 72 degrees, respectively. The contact angles corresponded to the critical surface tension of 31, 39 mJs^{-1} for PS, PMMA [13], respectively. Young's equation relates the contact angle, surface tension of the solid surface (γ_{SV}), surface tension of the liquid surface (γ_{LV}), and liquid–solid interfacial tension (γ_{SL}) [14]:

$$\gamma_{SV} = \gamma_{LV} \cos\theta + \gamma_{SL}. \quad (1)$$

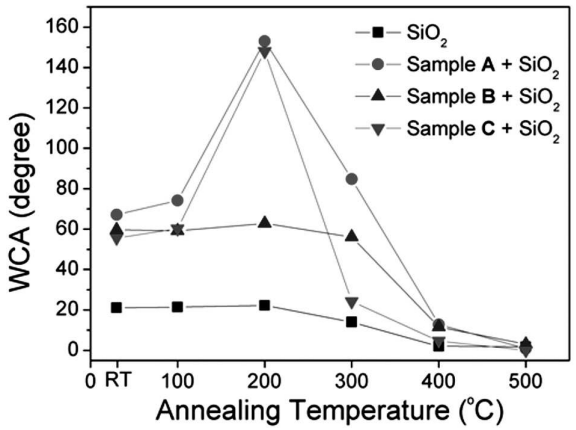

Fig. 2. Relationship between WCA of the composite films and the annealing temperature

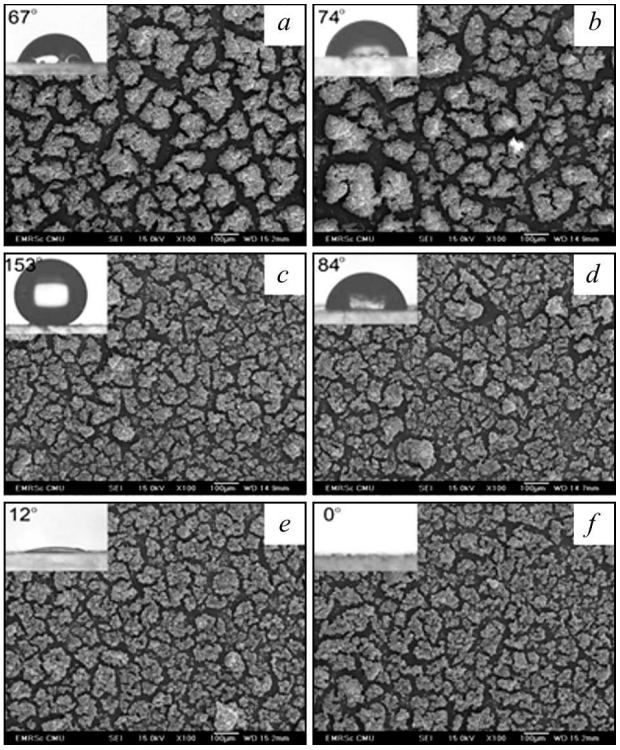

Fig. 3. SEM images and the WCAs (inset) of PS-SiO_2 nanocomposite films on a glass substrate; as-prepared (*a*) and annealed at 100 °C (*b*), 200 °C (*c*), 300 °C (*d*), 400 °C (*d*), and 500 °C (*f*)

From Eq. (1), it is found that the low surface energy on the solid surfaces provides high WCAs.

The WCA slightly decreases with the annealing temperature less than 200 °C. However, the WCA suddenly decreases at higher annealing temperature due to the thermal degradation to monomers which has the hydrophilic property [15–19]. Moreover, an increase in the surface roughness from the annealing treatment also causes a decrease of WCA.

Toluene solvent and solutions A–C were mixed with hydrophilic SiO_2 nanoparticles. After the dip coating process, all samples were annealed in air at various temperatures and showed WCA as a function of the annealing temperature (Fig. 2). The WCAs of SiO_2 coated on glass were less than 20 degrees for all annealing temperatures due to the water absorption of silica. For samples A–C, at the annealing temperature of 100 °C, the WCAs were in the interval of 60–80°. It was very interesting that the annealing at 200 °C switched samples A and C to superhydrophobicity at the WCA of 153° and 148°. In sharp contrast, sample B was still hydrophilic. However, as the annealing temperature higher than 200 °C the WCA for all samples rapidly decreased and presented the superhydrophilicity with WCA lower than 10 degrees at the annealing temperature of 500 °C. It is clearly seen that the PS-SiO_2 nanocomposite films show the best superhydrophobic properties and therefore were chosen for the further study.

Figure 3 shows the SEM images of dip-coated PS-SiO_2 nanocomposite films, and the water droplets on the surfaces are shown in the inset. For the films as-prepared and annealed at 100 °C, we see the island structure with a width of an order of a hundred micrometers. The results of image processing show that the area fractions of the films as-prepared and annealed at 100 °C were around 55%. The WCAs corresponding to the hydrophilicity were 67° and 74° for the films as-prepared and annealed at 100 °C. The area fraction then increased to 70% with an increase in the annealing temperature to 200 °C. This was due to the island expansion. At the annealing temperature of 200 °C, the film presented the superhydrophobic surface. It is well known that the suitable nanostructure surface together with wax-like materials result in the superhydrophobicity. The melting point of PS is 240 °C. Therefore, they were removed at the annealing temperature of 300–500 °C. The film turned to the hydrophilicity and superhydrophilicity with the WCA of 84°, 12°, and 0° for the annealing temperatures of 300 °C, 400 °C, and 500 °C, respectively.

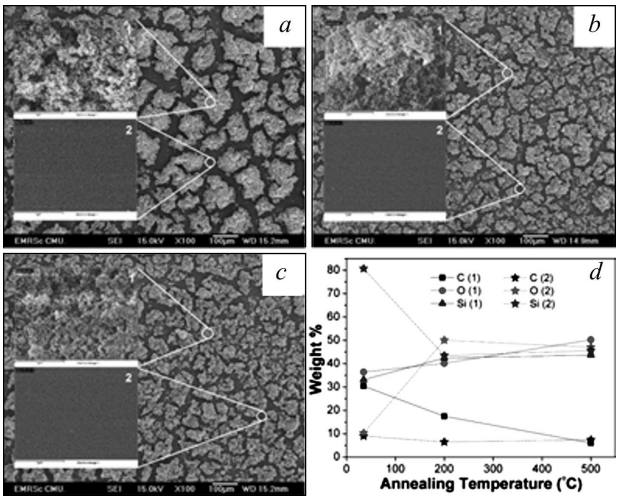

Fig. 4. SEM images of PS-SiO_2 nanocomposite films on a glass substrate at a high magnification; as-prepared (*a*) and annealed at 200 °C (*b*) and 500 °C (*c*). EDS (*d*) element weight percent of the composited films

Figure 4 shows SEM images at a high magnification of the as-deposited and samples annealed at 200 °C and 500 °C. The nanoparticles clearly seen are imbedded on the film islands and form the nanoscale roughness in all samples. These hierarchical structures, micro-protrusions, and nanostructures on the surfaces were similar to a natural lotus leaf [20]. Elemental weight percents of the nanocomposite films were investigated by EDS (shown in Fig. 4, *d*). C, O, and Si elemental peaks were observed at different ratios. It can be seen that, with increasing the annealing temperature, the C weight content ratio decreased, whereas the percentage ratios of O and Si increased. At the annealing temperature of 200 °C, the PS structure on the films was deformed and covered on the SiO_2 NPs to improve the surface roughness and hydrophobicity of the films [21]. As the annealing temperature was increased over the PS melting point (240 °C), the deformation of PS caused holes in the films, which increases the surface roughness (confirm by AFM). The water absorption of the remained silica and nanostructure surface provided superhydrophilic surfaces.

AFM images of the films as-prepared and annealing at 100, 200, 300, 400, and 500 °C are shown in Fig. 5, *a-f* with surface roughnesses of 22.39, 22.25, 29.17, 35.71, 39.37, and 45.32 nm, respectively. The surface roughness was increased dramati-

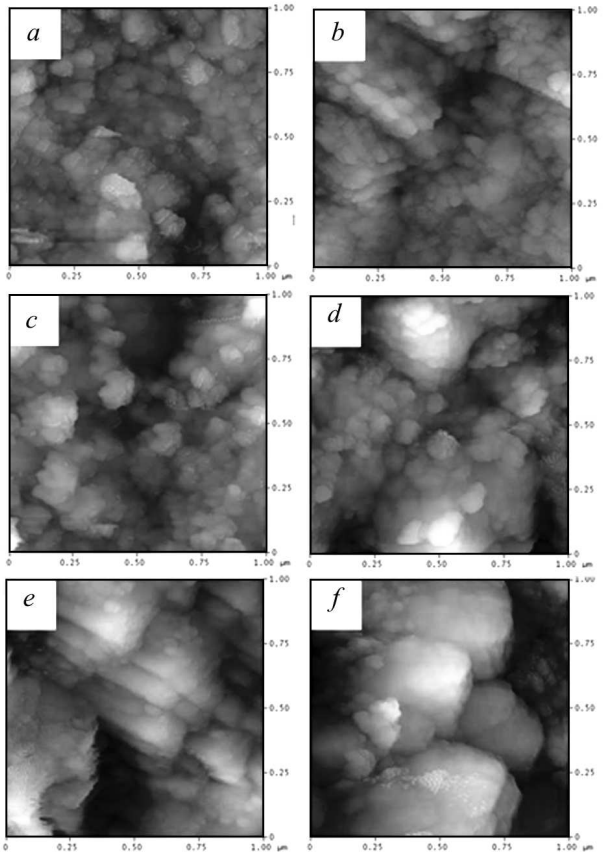

Fig. 5. AFM images of the PS-SiO_2 films as-prepared(*a*) and annealed at 100 °C (*b*), 200 °C (*c*), 300 °C (*d*), 400 °C (*e*), and 500 °C (*f*)

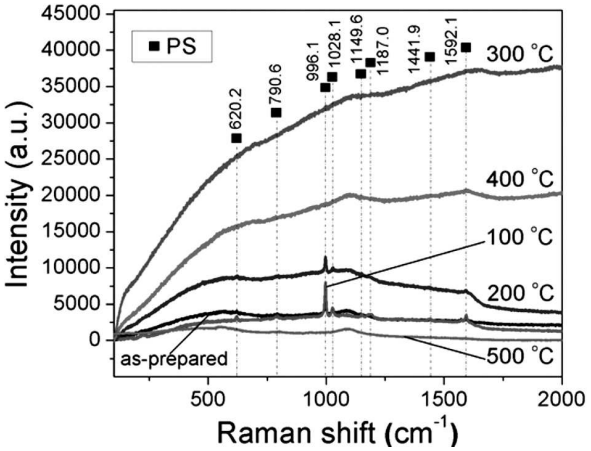

Fig. 6. Raman spectra of the as-prepared PS-SiO_2 and annealed films

cally at the annealing temperature ranging from 100 to 500 °C. This is due to the deformation of PS, but SiO_2 NPs still remain on the films.

The Raman spectra of the as-prepared PS-SiO_2 and annealed films were measured at room temperature, as shown in Fig. 6. The vibrational modes of aromatic rings in PS-SiO_2 were observed in the as-prepared and annealed SiO_2 films at 100 °C, which corresponded to the characteristic peaks of PS. The plane ring deformation modes were at 620.2 and 790.6 cm^{-1}. The symmetric C–C stretch or breathing mode of an aromatic ring was at 996.1 cm^{-1}. The C–H in-plane bending modes were at 1028.1, 1149.6, and 1187.0 cm^{-1}. The C–C stretching mode was at 1441.9 cm^{-1}, and the C–C quadrant stretching mode was at 1592 cm^{-1} [22–24]. However, the samples exhibited the high Raman fluorescence and the PS peaks disappeared upon the further increase in the annealing temperature to 500 °C. This result indicated the PS degradation, which correspondings to a low carbon content in the EDS analysis.

4. Conclusions

Superhydrophilic/superhydrophobic PS-SiO_2 nanocomposite films with island structures were prepared by the dip coating method. After being further annealed at 200 °C, the PS-SiO_2 coating acquired the superhydrophobicity with a WCA of 153 ° and became transparent. However, the films annealed at a high temperature (500 °C) showed the superhydrophilicity with the complete spreading of water. The results can significantly contribute to the development of changeable superhydrophobic/superhydrophilic coatings over large surface areas for industrial applications.

This work was supported by a Chiang Mai University (CMU) (new researcher grant 2014), Materials Science Research Center (MSRC), National Nanotechnology Center (NANOTEC), Thailand Research Fund (TRF), National Research University (NRU) Project under Thailand's office of the Commission on Higher Education (CHE), and the Graduate School in Chiang Mai University (GSCMU).

1. P. Patel, C.K. Choi, D.D. Meng. Superhydrophilic surfaces for antifoqging and antifouling microfluidic devices. *J. Assoc. Lab. Autom.* **15(2)**, 114 (2010).
2. W. Thongsuwan, T. Kumpika, P. Singjai. Effect of high roughness on a long aging time of superhydrophilic TiO_2 nanoparticle thin films. *Curr. Appl. Phys.* **11**, 1237 (2011).
3. R. Fürstner, W. Barthlott, C. Neinhuis, P. Walzel. Wetting and self-cleaning properties of artificial superhydrophobic surfaces. *Langmuir* **21**, 956 (2005).
4. S. Khorsand, K. Raeissi, F. Ashrafizadeh. Corrosion resistance and long-term durability of super-hydrophobic nickel film prepared by electrodeposition process. *Appl. Surf. Sci.* **305**, 498 (2014).
5. T. Kako, A. Nakajima, H. Irie, Z. Kato, K. Uematsu, T. Watanabe, K. Hashimoto. Adhesion and sliding of wet snow on a super-hydrophobic surface with hydrophilic channels. *J. Mater. Sci.* **39**, 547 (2004).
6. W. Intarasang, W. Thamjaree, D. Boonyawan, W. Nhuapeng. Effect of coating time on LPP treated silk fabric coated with ZnO_2 nanoparticles. *Chiang Mai J. Sci.* **40(6)**, 1000 (2013).
7. E.N. Miller, D.C. Palm, D.D. Silva, A. Parbatani, A.R. Meyers, D.L. Williams, D.E. Thompson. Microsphere lithography on hydrophobic surfaces for generating gold films that exhibit infrared localized surface plasmon resonances. *J. Phys. Chem.* B **117**, 15313 (2013).
8. A.M. Coclite, Y. Shi, K.K. Gleason. Super-hydrophobic and oloephobic crystalline coatings by initiated chemical vapor deposition. *Phys. Procedia* **46**, 56 (2013)
9. S. Liu, S.S. Latthe, H. Yang, B. Liu, R. Xing. Raspberry-like superhydrophobic silica coatings with self-cleaning properties. *Ceramics Inter.* **41(9)**, 11719 (2015).
10. D. Lopez-Torres, C. Elosua, M. Hernaez, J. Goicoechea, F.J. Arregui. From superhydrophilic to superhydrophobic surfaces by means of polymeric Layer-by-Layer films. *Appl. Surf. Sci.* **351**, 1081 (2015).
11. J. Liang, K. Liu, D. Wang, H. Li, P. Li, S. Li, S. Su, S. Xu, Y. Luo. Facile fabrication of superhydrophilic/superhydrophobic surface on titanium substrate by single-step anodization and fluorination. *Appl. Surf. Sci.* **338**, 126 (2015).
12. Y.H. Lin, K.L. Su, P.S. Tsai, F.L. Chuang, Y.M. Yang. Fabrication and characterization of transparent superhydrophilic/superhydrophobic silica nanoparticulate thin films. *Thin Solid Films* **519**, 5450 (2011).
13. F.M. Fowkes. Attractive forces at interfaces. *Ind. Eng. Chem.* **56**, 40 (1964).
14. K.Y. Law, H. Zhao. *Surface Wetting: Characterization, Contact Angle, and Fundamentals.* (Springer, 2015) [ISBN: 978-3-319-25214-8].
15. T. Faravelli, M. Pinciroli, F. Pisano, G. Bozzano, M. Dente, E. Ranzi. Thermal degradation of polystyrene. *J. Anal. Appl. Pyrolysis* **60**, 103 (2001).
16. J.D. Peterson, S. Vyazovkin, C.A. Wight. Kinetics of the thermal and thermo-oxidative degradation of polystyrene, polyethylene and poly(propylene). *Macromol. Chem. Phys.* **202**, 775 (2001).
17. Y.H. Hu, C.Y. Chen. Study of the thermal behaviour of poly(methyl methacrylate) initiated by lactams and thiols. *Polym. Degrad. Stab.* **80**, 1 (2003).
18. Y.H. Hu, C.Y. Chen. The effect of end groups on the thermal degradation of poly(methyl methacrylate). *Polym. Degrad. Stab.* **82**, 81 (2003).

19. M. Ferriol, A. Gentilhomme, M. Cochez, N. Oget, J.L. Mieloszynski. Thermal degradation of poly(methyl methacrylate) (PMMA): modelling of DTG and TG curves. *Polym. Degrad. Stab.* **79**, 271 (2003).
20. A. Otten, S. Herminghaus. How plants keep dry: A physicist's point of view. *Langmuir* **20(6)**, 2405 (2004).
21. W. Hou, Q. Wang. Wetting behavior of a SiO_2–polystyrene nanocomposite surface. *J. Colloid Interface Sci.* **316**, 206 (2007).
22. J.R. Anema, A.G. Brolo, A. Felten, C. Bittencourt. Surface-enhanced Raman scattering from polystyrene on gold clusters. *J. Raman Spectrosc.* **41**, 745 (2010).
23. W.M. Sears, J.L. Hunt, J.R. Stevens. Raman scattering from polymerizing styrene. I. Vibrational mode analysis. *J. Chem. Phys.* **75(4)**, 1589 (1981).
24. D.B. Menezes, A. Reyer, A. Marletta, M. Musso. Glass transition of polystyrene (PS) studied by Raman spectroscopic investigation of its phenyl functional groups. *Mater. Res. Express.* **754(1)**, 015303 (2017).

Received 28.12.17

А. Срібнруанг, Т. Кумпіка, В. Сроіла,
Е. Кантарак, П. Сінгджай, В. Тхонгсуван

ПЕРЕТВОРЕННЯ ПРОЗОРИХ ПЛІВОК НАНОКОМПОЗИТІВ ПС-ПММА-SiO_2 ВІД СУПЕРГІДРОФОБНОСТІ ДО СУПЕРГІДРОФІЛЬНОСТІ

Р е з ю м е

Виготовлено прозоре супергідрофобне нанопокриття простим крапельним шляхом. Контактний кут з водою >150°. Розчини для покриття приготовлені розчиненням полістирола (ПС) і полиметилметакрилата в толуолі. Для збільшення шорсткості покриття додавався диспергований кремнезем SiO_2. Підібрано умови відпалу і інші чинники для оптимізації прозорості та кута контакту з водою на плівці. Досліджено вплив температури відпалу на плівки. Супергідрофобність спостерігалася лише в ПС-плівках після відпалу при 200 °С. Перехід від супергідрофобності до супергідрофільності спостерігався при температурах відпалу вище 200 °С завдяки розпаду полімеру на гідрофільні мономери.